

# Demonstration of chalcogenide glass racetrack micro-resonators

Juejun Hu,<sup>1,\*</sup> Nathan Carlie,<sup>2</sup> Laetitia Petit,<sup>2</sup> Anu Agarwal,<sup>1</sup> Kathleen Richardson,<sup>2</sup> and  
Lionel Kimerling<sup>1</sup>

<sup>1</sup>*Microphotonics Center, Massachusetts Institute of Technology, Cambridge, MA 02139, USA*

<sup>2</sup>*Advanced Materials Research Laboratory, Clemson University, Anderson, SC 29625, USA*

\*Corresponding author: [hujuejun@mit.edu](mailto:hujuejun@mit.edu)

We have demonstrated the first chalcogenide glass racetrack micro-resonator using a CMOS-compatible lift-off technique with thermally evaporated As<sub>2</sub>S<sub>3</sub> films. The device features a small footprint of 0.012 mm<sup>2</sup>, a cavity Q (quality factor) of 10,000 and an extinction ratio of 32 dB, simultaneously. These resonators exhibit a very high sensitivity to refractive index changes, with a demonstrated detection capability of  $\Delta n_{\text{As}_2\text{S}_3} = (4.5 \times 10^{-6} \pm 10\%) \text{ RIU}$  (Refractive Index Unit). The resonators were applied to derive photorefractive response of As<sub>2</sub>S<sub>3</sub> to  $\lambda = 550 \text{ nm}$  light. The resonator devices are a versatile platform for both sensing and glass material property investigation. © 2007 Optical Society of America

*OCIS codes:* 130.3120, 130.2755, 130.4310, 130.6010, 160.2750, 190.5330.

In an optical resonator, circulating light is confined within a small volume. When the resonant condition is met, the optical power becomes resonantly enhanced up to a factor approximating cavity finesse. Such resonant enhancement, combined with a significantly increased optical path length, makes ring and racetrack resonators an ideal device platform for both fundamental investigations and practical applications based on photon-matter interactions. The examples include all-optical switching<sup>1</sup>, light emission<sup>2</sup>, nonlinear optics<sup>3</sup>, and biochemical sensing<sup>4</sup>. Chalcogenide (ChG) glasses have been identified to be a promising material candidate for the aforementioned applications due to their unique optical properties in the infrared. Of particular relevance here are the photosensitivity, reduced phonon quenching, large Kerr optical non-linearity, and wide infrared transparency window<sup>5</sup> of ChG materials. Thus, a micro-resonator in chalcogenide glasses that maximizes the leverage of their properties becomes highly desirable.

Here we present the first demonstration of chalcogenide glass racetrack resonators in thermally evaporated  $\text{As}_2\text{S}_3$  films. We have also shown that such resonators can be used as ultra-sensitive probes of photosensitivity in chalcogenide glass, providing unprecedented high accuracy measurement (on the order of  $10^{-6}$  RIU) of photorefractive index change.

The bulk preparation and film deposition process are described elsewhere<sup>6, 7</sup>. These devices were patterned by lift-off, and the whole patterning process has been carried out on a 500 nm CMOS line<sup>8</sup>. The CMOS-compatibility allows this process to be scaled up for mass production. The racetracks are comprised of strip waveguides with a width of 800 nm and a height of 450 nm. After patterning, a layer of 3  $\mu\text{m}$  thick SU8 polymer was spin-coated to serve as the top cladding. The device was subsequently annealed at 130°C for 3 hours to stabilize the glass structure. Figure 1 shows the top view of a fabricated resonator. The fabricated device has a small footprint of 0.012  $\text{mm}^2$ , and the total cavity length is  $\sim 409 \mu\text{m}$ .

Transmission spectra of the fabricated device have been measured on a Newport AutoAlign workstation in combination with a tunable laser (optical vector analyzer external laser, LUNA Technologies, Inc.). Lens-tip fibers are used to couple light from the laser into and out of the devices. Reproducible coupling is achieved via an automatic alignment system with a spatial resolution of 50 nm. The sample was mounted on a thermostat stage and kept at 25 °C for all measurements. Figure 2(a) shows a measured transmission spectrum of TM polarization. The resonator has a Free Spectral Range (FSR) of 2.5 nm and a maximum extinction ratio of 32 dB near 1550 nm. Such a high extinction ratio indicates that the resonator works near the critical coupling regime. Cavity Q, defined as the ratio of wavelength against 3 dB resonant peak width, was determined from Fig. 2(b) to be ~10,000. This Q value corresponds to an equivalent waveguide loss of 16.5 dB/cm. We expect that an optimized fabrication process with minimized pattern digitization error of waveguide bends, post-fabrication smoothing and GRIN waveguide design<sup>9</sup> could further reduce waveguide loss, leading to even higher Q factors. For comparison, photonic crystal cavities in Ge<sub>33</sub>As<sub>12</sub>Se<sub>55</sub> chalcogenide glass have recently been demonstrated with a similar Q of 10,000 and an extinction ratio up to 2.6 dB<sup>10</sup>.

An important feature of resonators is their extreme sensitivity to refractive index changes, and thus they have been proposed to be a promising candidate for miniaturized biochemical sensors<sup>11</sup>. This property can also be utilized to probe micro-structural evolution in chalcogenide glasses, since structural modifications in these glasses are often accompanied by a refractive index change<sup>12</sup>. In addition, accurate determination of the index change is also technically important for applications that rely on photo-induced index modifications such as direct laser writing. For example, Zoubir et al. measured an index increase up to 0.08 at 785 nm wavelength in femtosecond laser written As<sub>2</sub>S<sub>3</sub> waveguides<sup>13</sup>. Often, the spectrum from a single scan has low

Signal-to-Noise Ratio (SNR) and does not allow accurate determination of index change. For this reason, we have used multiple scan averaging over a single resonant peak to improve SNR and wavelength resolution. By averaging over 64 individual scans, noise in the transmission spectrum is suppressed, as is evident in Fig. 2(b).

To study the photosensitivity of  $\text{As}_2\text{S}_3$ , the resonator device was exposed to timed near-bandgap light ( $\sim 550$  nm wavelength with an irradiance of  $6.2 \text{ mW/cm}^2$  from a band pass filtered halogen lamp) to induce a controlled refractive index change using a setup schematically shown in Fig. 3(a), and the resulting peak shift was monitored in-situ. A Lorentzian fit has been used to extract the accurate peak position. Refractive index change can be calculated via:

$$\Delta n = \frac{\Delta \lambda}{\lambda} \times n_g / \Gamma \quad (1)$$

where  $\Delta \lambda$  stands for the resonant peak shift,  $n_{\text{eff}}$  is the waveguide effective index, and  $\Gamma$  is the confinement factor in  $\text{As}_2\text{S}_3$  core. Finite-difference simulations give  $n_{\text{eff}}$  and  $\Gamma$  of TM polarization to be 1.88 and 0.77, respectively.

Figure 3(b) gives an example of two spectra with a peak shift of  $(3 \pm 0.3) \text{ pm}$  after light exposure, corresponding to an index increase of  $4.5 \times 10^{-6} \pm 10\%$  in  $\text{As}_2\text{S}_3$  at 1597 nm wavelength. The wavelength resolution of 0.3 pm was statistically determined by repeating the experiment and comparing multiple measurement results. Such a high sensitivity is essential especially for accurate photosensitivity measurement in annealed glass, which exhibits much smaller photo-induced index change compared to its as-deposited counterpart<sup>14</sup>.

Figure 4 shows the refractive index increase at 1550 nm wavelength as a function of exposure dose for both as-deposited (without annealing) and annealed  $\text{As}_2\text{S}_3$  devices. Excellent

data reproducibility was confirmed by repeating the measurement on several resonators. In both cases the index increase can be well described with a single-exponential function:

$$\Delta n = \Delta n_{sat} \times [1 - \exp(-D / D_0)] \quad (2)$$

where  $\Delta n_{sat}$  is the maximum index change when the photorefractive effect has been fully saturated,  $D$  represents the exposure dose in  $\text{J}/\text{cm}^2$  and  $D_0$  is a material constant which depends on processing history. Our results confirm the validity of exponential empirical fit in previous reports<sup>15, 16</sup>. For unannealed  $\text{As}_2\text{S}_3$ ,  $\Delta n_{sat} = 0.0505 \pm 0.0002$ ,  $D_0 = (0.036 \pm 0.001) \text{ J}/\text{cm}^2$ , whereas for annealed  $\text{As}_2\text{S}_3$ ,  $\Delta n_{sat} = 0.0125 \pm 0.0001$ ,  $D_0 = (0.024 \pm 0.001) \text{ J}/\text{cm}^2$ . The smaller photo-induced index change in annealed glass has also been observed by C. Lopez in  $\text{As}_2\text{S}_3$  films prepared by the same deposition technique, irradiated with an 800 nm femtosecond laser and measured using an ellipsometer<sup>14</sup>.

It is also important to note that the annealed and unannealed samples have distinctive  $D_0$  values, which indicate different micro-structural modifications. This finding confirms that photo-saturated state and thermally annealed state are structurally dissimilar in chalcogenide glasses<sup>14, 17</sup>.

To summarize, we have demonstrated the first chalcogenide glass racetrack micro-resonator in thermally evaporated  $\text{As}_2\text{S}_3$  film with a Q factor of 10,000 and an extinction ratio of 32 dB, providing a versatile platform for nonlinear optics, light emission and sensing using chalcogenide materials. These devices can detect refractive index change as small as  $4.5 \times 10^{-6}$  in  $\text{As}_2\text{S}_3$  with good SNR, and thus are also useful tools for probing micro-structural evolution in glasses.

## **Acknowledgment**

Funding support is provided by the Department Of Energy under award number DE-SC52-06NA27341. The authors also acknowledge the Microsystems Technology Laboratories at MIT for fabrication facilities.

## **Disclaimer**

This paper was prepared as an account of work supported by an agency of the US Government. Neither the US Government nor any agency thereof, nor any of their employees, makes any warranty or assumes any legal liability or responsibility for the accuracy, completeness or usefulness of any information, apparatus or process disclosed, or represents that its use would not infringe privately owned rights. Reference herein to any specific commercial product, process, or service by trade name, trademark, manufacturer, or otherwise does not necessarily constitute or imply its endorsement or favoring by the US Government. The opinions of authors expressed herein do not necessarily reflect those of the US Government or any agency thereof.

## **References**

1. V. Almeida, C. Barrios, R. Panepucci, and M. Lipson, "All-optical control of light on a silicon chip," *Nature* **431**, 1081 (2004).
2. J. Galas, J. Torres, M. Belotti, Q. Kou, and Y. Chen, "Microfluidic tunable dye laser with integrated mixer and ring resonator," *Appl. Phys. Lett.* **86**, 264101 (2005).
3. Q. Xu, V. Almeida, and M. Lipson, "Micrometer-scale all-optical wavelength converter on silicon," *Opt. Lett.* **30**, 2733 (2005).

4. K. De Vos, I. Bartolozzi, E. Schacht, P. Bienstman, and R. Baets, "Silicon-on-Insulator microring resonator for sensitive and label-free biosensing," *Opt. Express* **15**, 7610 (2007).
5. A. Greer and N. Nathur, "Materials science: Changing face of the chameleon," *Nature* **437**, 1246 (2005).
6. W. Li, S. Seal, C. Rivero, C. Lopez, K. Richardson, A. Pope, A. Schulte, S. Myneni, H. Jain, K. Antoine, and A. Miller, "Role of S/Se ratio in chemical bonding of As–S–Se glasses investigated by Raman, x-ray photoelectron, and extended x-ray absorption fine structure spectroscopies," *J. Appl. Phys.* **98**, 053503 (2005).
7. J. Hu, V. Tarasov, N. Carlie, L. Petit, A. Agarwal, K. Richardson, and L. Kimerling, "Fabrication and Testing of Planar Chalcogenide Waveguide Integrated Microfluidic Sensor," *Opt. Express* **15**, 2307 (2007).
8. J. Hu, V. Tarasov, N. Carlie, N. Feng, L. Petit, A. Agarwal, K. Richardson, and L. Kimerling, "Si-CMOS-compatible lift-off fabrication of low-loss planar chalcogenide waveguides," *Opt. Express* **15**, 11798 (2007).
9. J. Hu, N. Feng, N. Carlie, J. Wang, L. Petit, A. Agarwal, K. Richardson, and L. Kimerling, "Low-loss high-index-contrast planar waveguides with graded-index cladding layers," *Opt. Express* **15**, 14566 (2007).
10. Y. Ruan, M. Kim, Y. Lee, B. Luther-Davies, A. Rode, "Fabrication of high-Q chalcogenide photonic crystal resonators by e-beam lithography," *Appl. Phys. Lett.* **90**, 071102 (2007).
11. R. Boyd, and J. Heebner, "Sensitive Disk Resonator Photonic Biosensor," *Appl. Opt.* **40**, 5742 (2001).

12. J. Laniel, J. Ménarda, K. Turcotte, A. Villeneuve, R. Vallée, C. Lopez, and K. Richardson, "Refractive index measurements of planar chalcogenide thin film," *J. Non-Cryst. Solids* **328**, 183 (2003).
13. A. Zoubir, M. Richardson, C. Rivero, A. Schulte, C. Lopez, K. Richardson, N. Ho, and R. Vallée, "Direct femtosecond laser writing of waveguides in  $\text{As}_2\text{S}_3$  thin films," *Opt. Lett.* **29**, 748 (2004).
14. C. Lopez, "Evaluation of the photo-induced structural mechanisms in chalcogenide glass," University of Central Florida Ph.D Thesis (2004).
15. A. van Popta, R. DeCorby, C. Haugen, T. Robinson, J. McMullin, D. Tonchev, and S. Kasap, "Photoinduced refractive index change in  $\text{As}_2\text{Se}_3$  by 633nm illumination," *Opt. Express* **10**, 639 (2002).
16. M. Lee, C. Grillet, C. Smith, D. Moss, B. Eggleton, D. Freeman, B. Luther-Davies, S. Madden, A. Rode, Y. Ruan, and Y. Lee, "Photosensitive post tuning of chalcogenide photonic crystal waveguides," *Opt. Express* **15**, 1277 (2007).
17. H. Fritzsche, "Toward understanding the photoinduced changes in chalcogenide glasses," *Semiconductors* **32**, 850 (1998).



Fig. 1. Optical micrograph of a fabricated resonator device; inset SEM micrograph shows the coupling region between the coupling (bus) waveguide and the racetrack.

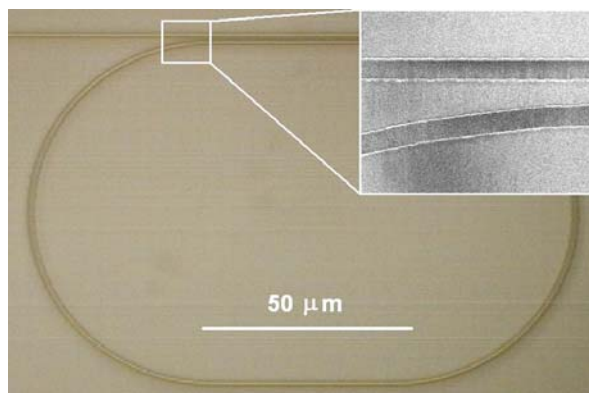


Fig. 2. Transmission spectra of TM polarization in a resonator device: (a) the resonator exhibits an FSR of 2.5 nm and an extinction ratio of 32 dB; (b) the resultant spectrum averaged over 64 consecutive scans.

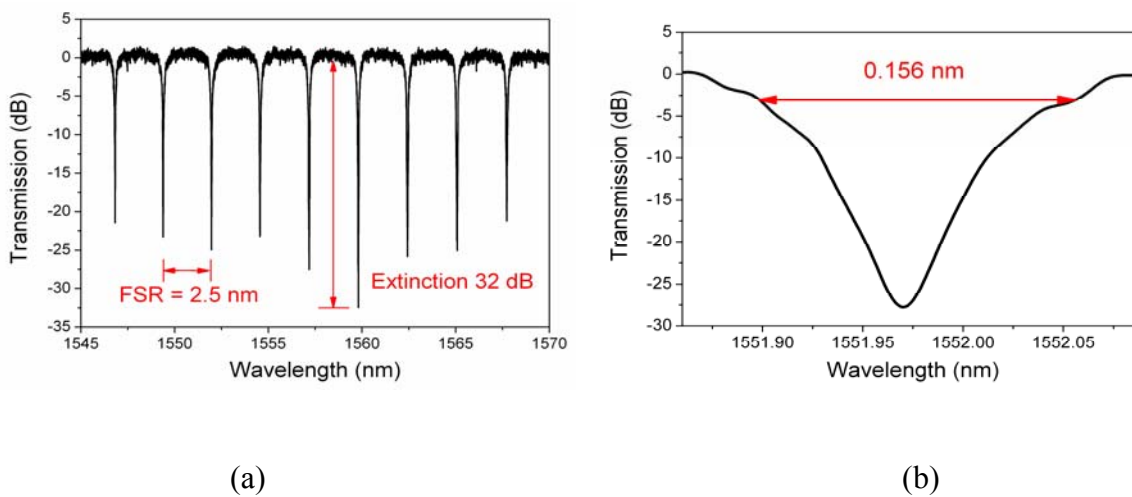


Fig. 3. (a) Photosensitivity measurement setup; (b) Transmission spectra of a resonator in the proximity of its resonant peak. Black dots represent experimental data points, and the red dots are data measured in the same device after exposure to ~550 nm wavelength light; the curves are

fitted Lorentzian peaks. A wavelength shift of  $(3 \pm 0.3)$  pm is determined by peak fit, corresponding to an index change of  $(4.5 \times 10^{-6} \pm 10\%)$  RIU in  $\text{As}_2\text{S}_3$  at 1597 nm wavelength.

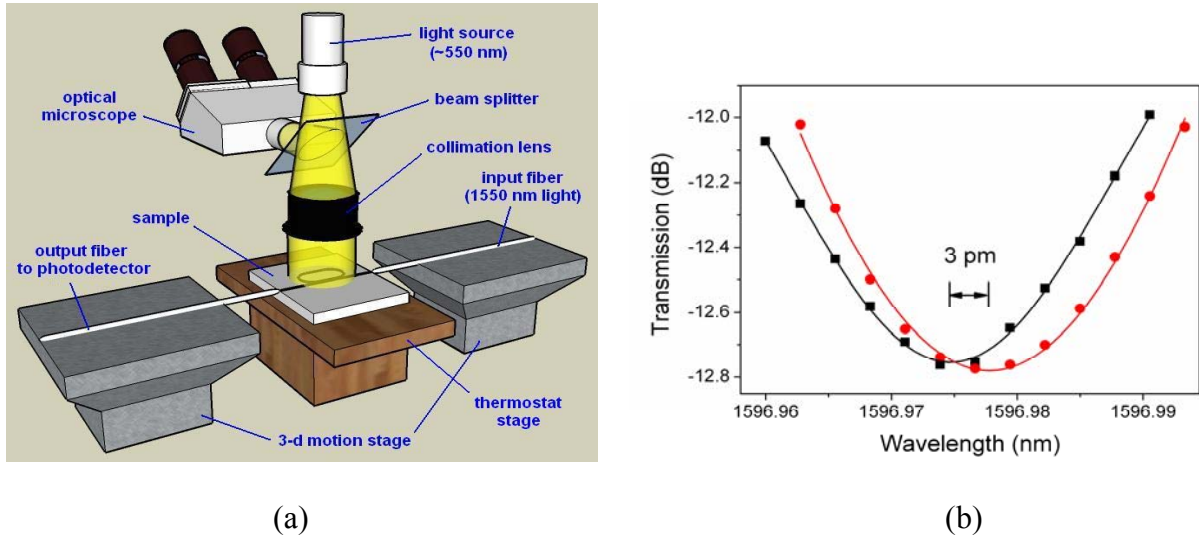


Fig. 4. Photo-induced refractive index change as a function of exposure dose ( $\lambda = 550$  nm) in an as-deposited, unannealed resonator and in a resonator annealed at  $130^\circ\text{C}$  for 3 hours

